Supporting Information for *Acta Phys. -Chim. Sin.* doi: 10.3866/PKU.WHXB202011012

基于ReaxFF的甲烷无氧转化气相机理研究

刘源[1,2,3]，段增晖[2]，李隽[2,3]，常春然[1,*]

[1] 西安交通大学化学工程与技术学院，陕西省能源化工过程重点实验室，西安 710049

[2] 清华大学化学系，有机光电子与分子工程教育部重点实验室，北京 100084

[3] 南方科技大学化学系，广东 深圳 518055

Gas-Phase Mechanism Study of Methane Nonoxidative Conversion by ReaxFF Method

Yuan Liu [1,2,3], Zenghui Duan [2], Jun Li [2,3], Chunran Chang [1,*]

[1] Shaanxi Key Laboratory of Energy Chemical Process Intensification, School of Chemical Engineering and Technology, Xi'an Jiaotong University, Xi'an 710049, China.

[2] Key Laboratory of Organic Optoelectronics & Molecular Engineering of Ministry of Education, Department of Chemistry, Tsinghua University, Beijing 100084, China.

[3] Department of Chemistry, Southern University of Science and Technology, Shenzhen 518055, Guangdong Province, China.

[*]Corresponding author. Email: changcr@mail.xjtu.edu.cn.

Simulation Results

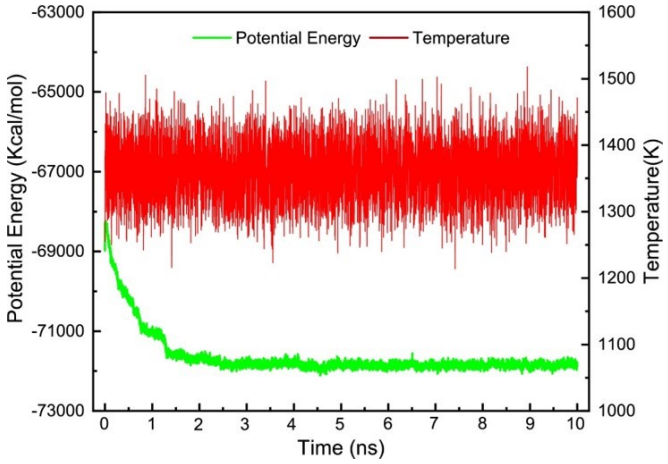

Fig. S1 The temperature and potential energy of the CH_4(80)/CH_3·(80)/H_2(40) gas-phase system as a function of time in the first parallel simulation.

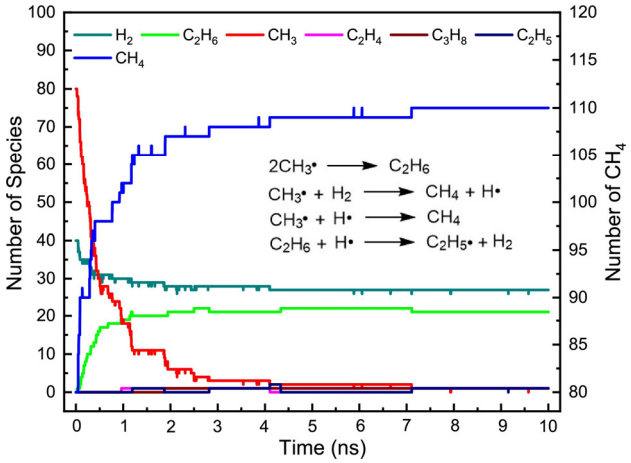

Fig. S2 Products distribution of the second parallel simulation beginning from the CH_4(80)/CH_3·(80)/H_2(40) gas-phase system as a function of time.

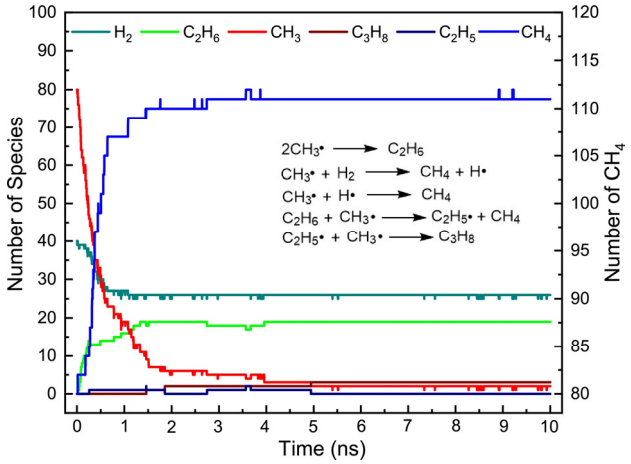

Fig. S3 Products distribution of the third parallel simulation beginning from the CH_4(80)/CH_3·(80)/H_2(40) gas-phase system as a function of time.

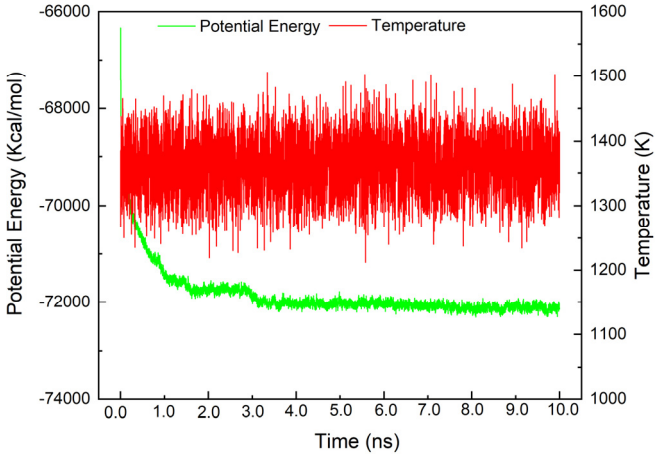

Fig. S4 The temperature and potential energy of the CH_4(80)/CH_3·(80)/H_2(20)/H·(40) gas-phase system as a function of time in the first parallel simulation.

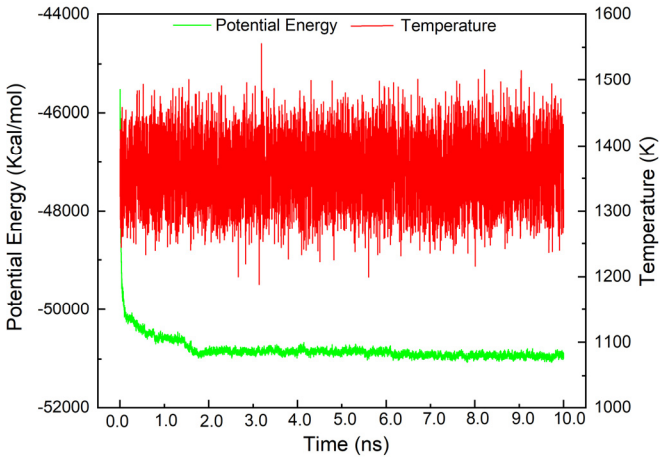

Fig. S5 The temperature and potential energy of the CH_4(100)/H·(100) gas-phase system as a function of time in the first parallel simulation.

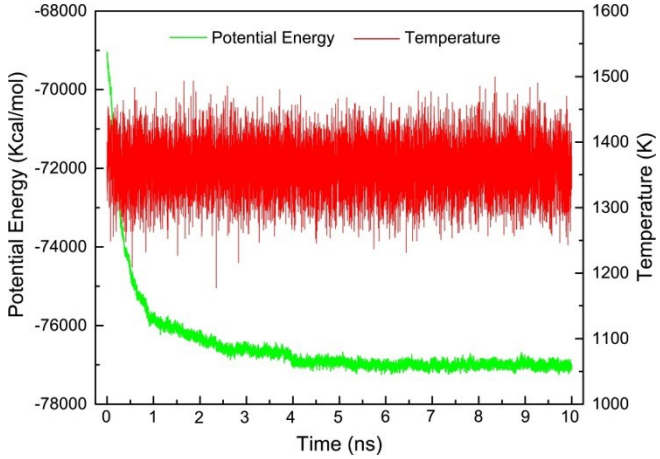

Fig. S6 The temperature and potential energy of the CH_3·(200) gas-phase system as a function of time in the first parallel simulation.

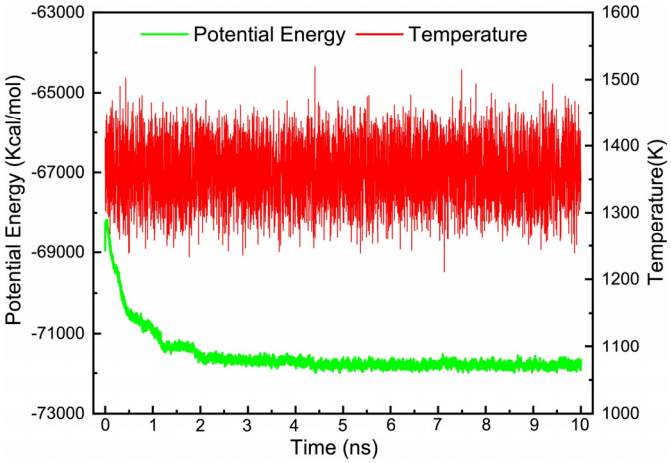

Fig. S7 The temperature and potential energy of the CH_4(80)/CH_3·(80)/H_2(40) gas-phase system as a function of time in the second parallel simulation.

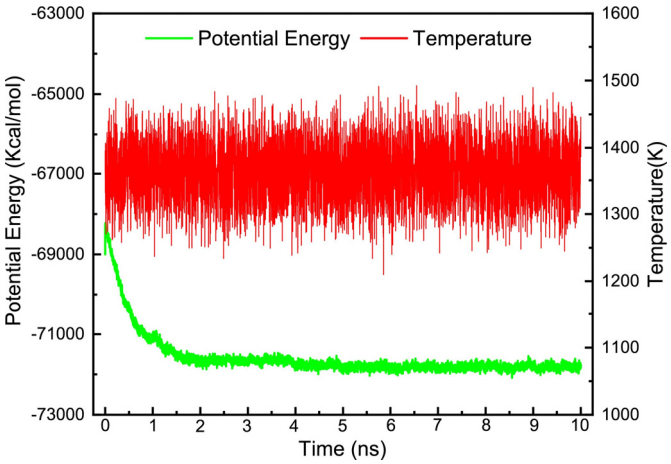

Fig. S8 The temperature and potential energy of the CH_4(80)/CH_3·(80)/H_2(40) gas-phase system as a function of time in the third parallel simulation.

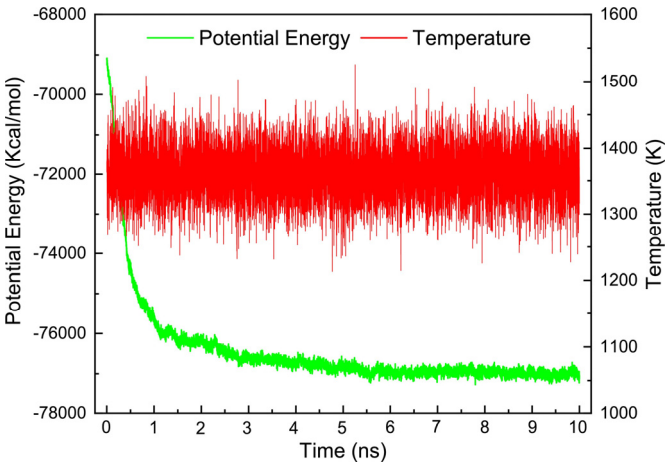

Fig. S9 The temperature and potential energy of the CH_3·(200) gas-phase system as a function of time in the second parallel simulation.

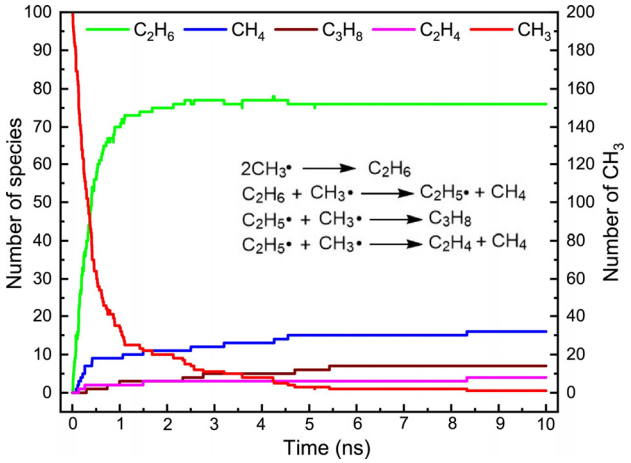

Fig. S10 Products distribution of the second parallel simulation beginning from the CH_3·(200) gas-phase system as a function of time.

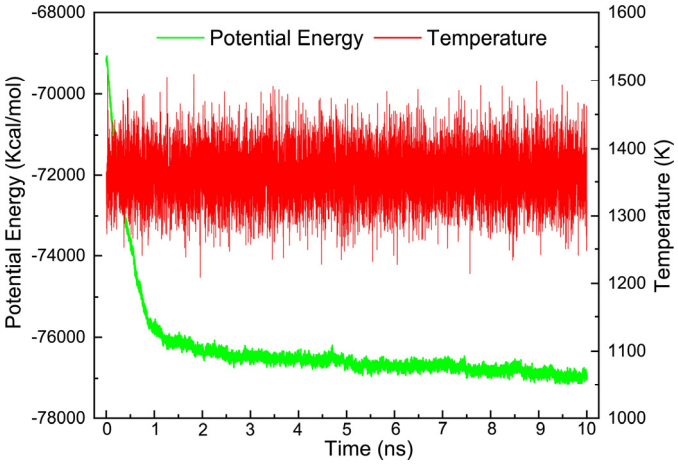

Fig. S11 The temperature and potential energy of the CH_3·(200) gas-phase system as a function of time in the third parallel simulation.

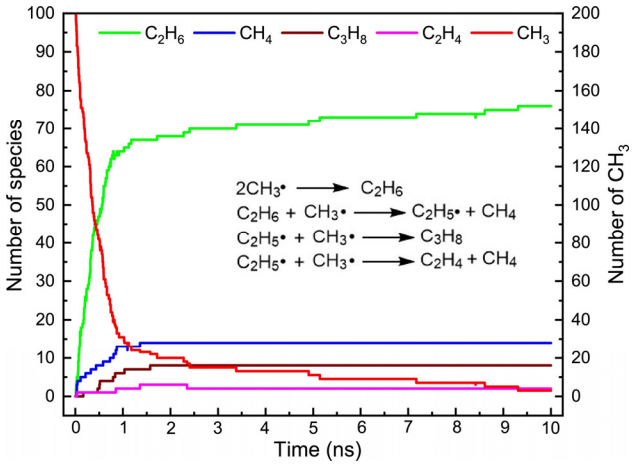

Fig. S12 Products distribution of the third parallel simulation beginning from the CH_3·(200) gas-phase system as a function of time.

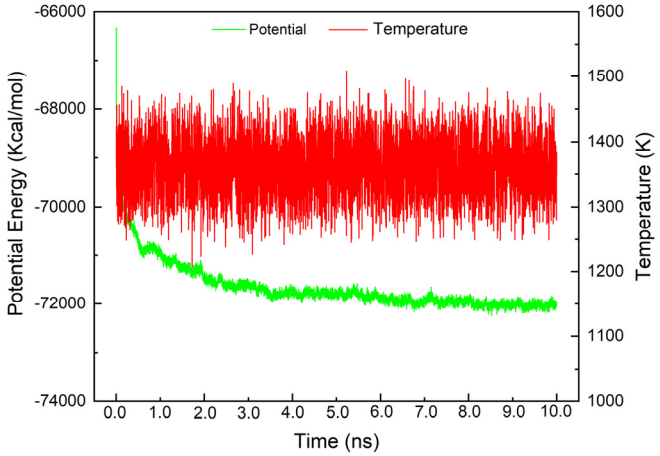

Fig. S13 The temperature and potential energy of the CH_4(80)/CH_3·(80)/H_2(20)/H·(40) gas-phase system as a function of time in the second parallel simulation.

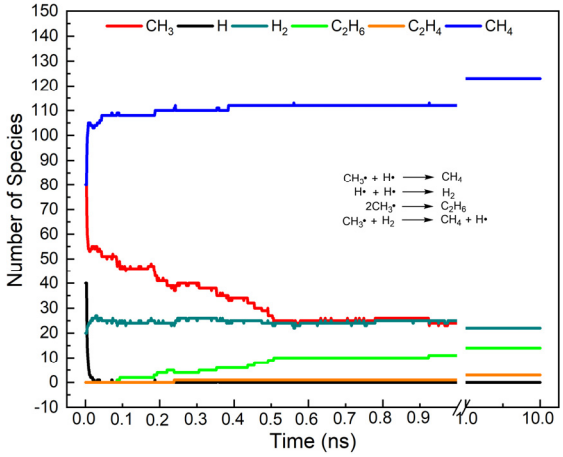

Fig. S14 Products distribution of the second parallel simulation beginning from the CH_4(80)/CH_3·(80)/H_2(20)/H·(40) gas-phase system as a function of time.

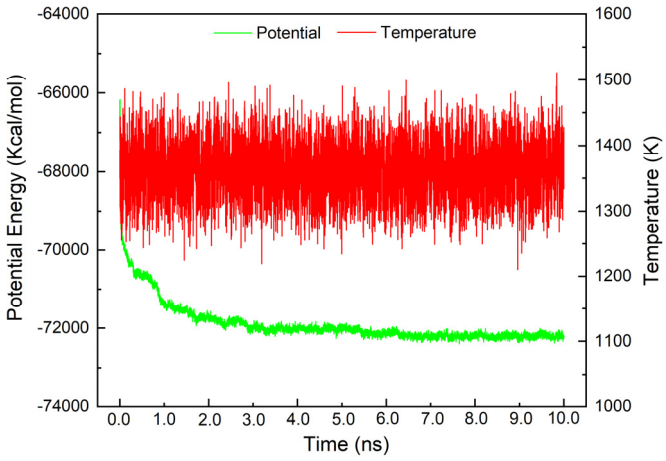

Fig. S15 The temperature and potential energy of the CH_4(80)/CH_3·(80)/H_2(20)/H·(40) gas-phase system as a function of time in the third parallel simulation.

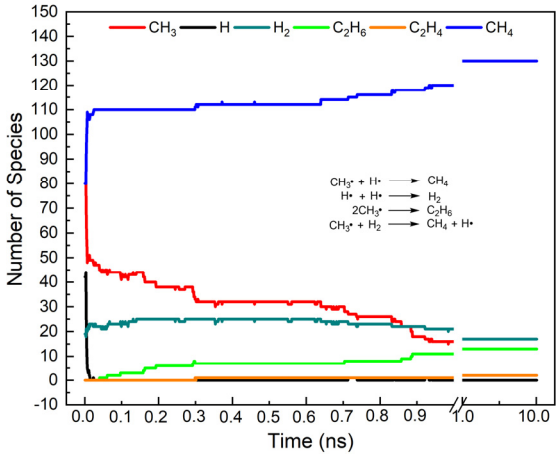

Fig. S16 Products distribution of the third parallel simulation beginning from the CH_4(80)/CH_3·(80)/H_2(20)/H·(40) gas-phase system as a function of time.

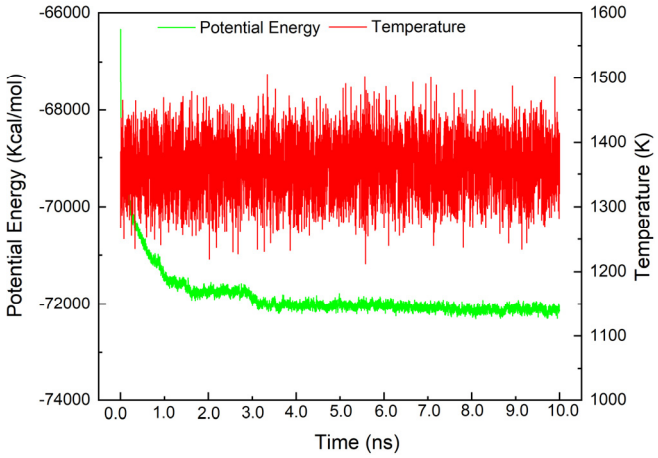

Fig. S17 The temperature and potential energy of the CH_4(100)/H·(100) gas-phase system as a function of time in the second parallel simulation.

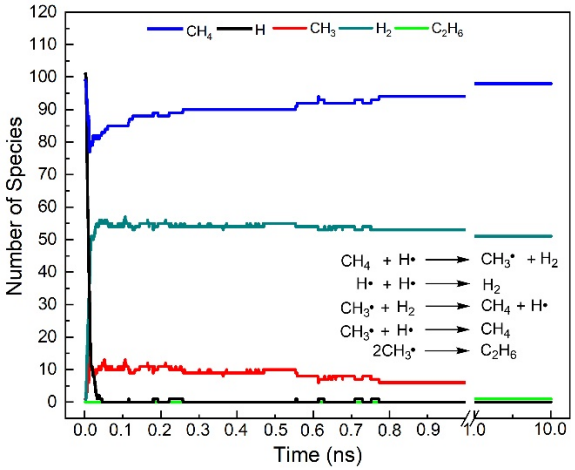

Fig. S18 Products distribution of the second parallel simulation beginning from the CH_4(100)/H·(100) gas-phase system as a function of time.

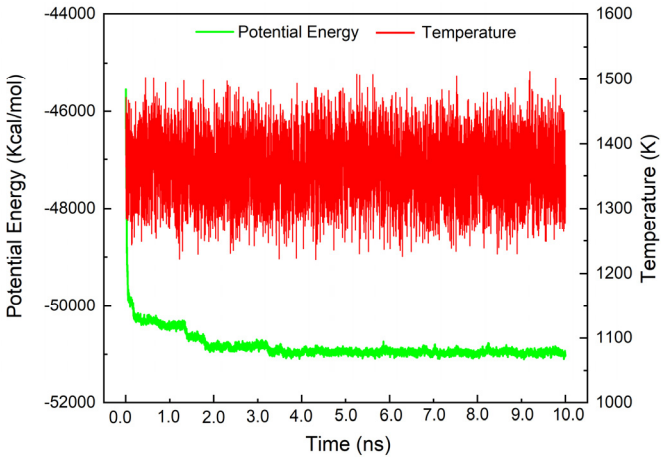

Fig. S19 The temperature and potential energy of the CH_4(100)/H·(100) gas-phase system as a function of time in the third parallel simulation.

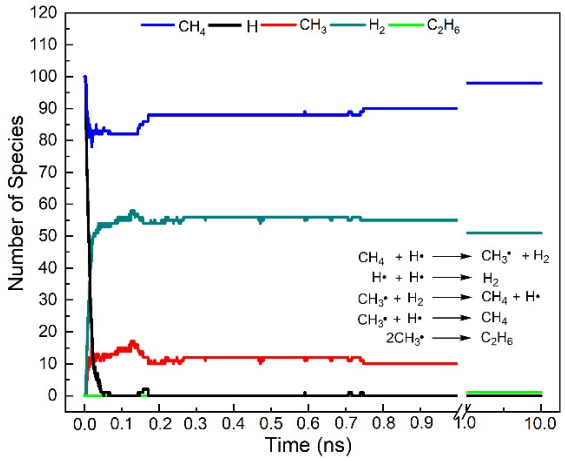

Fig. S20 Products distribution of the third parallel simulation beginning from the CH_4(100)/H·(100) gas-phase system as a function of time.

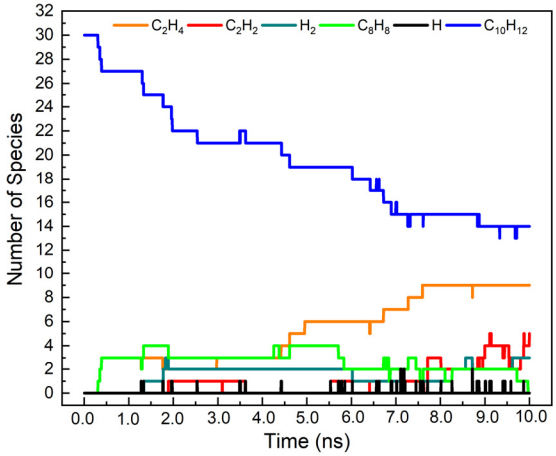

Fig. S21 Products distribution of the second parallel simulation beginning from the $C_{10}H_{12}$(30) system at 1500 K as a function of time.

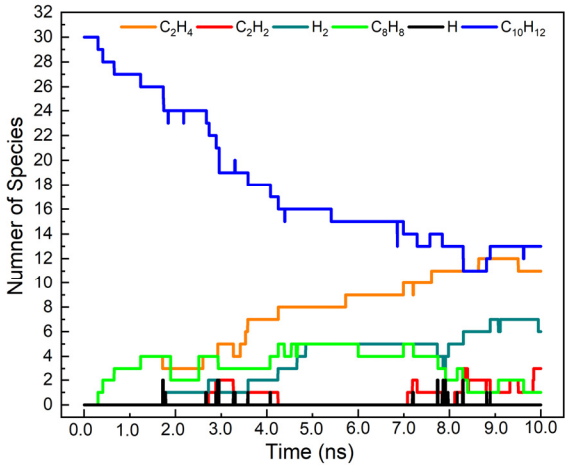

Fig. S22 Products distribution of the third parallel simulation beginning from the $C_{10}H_{12}$(30) system at 1500 K as a function of time.

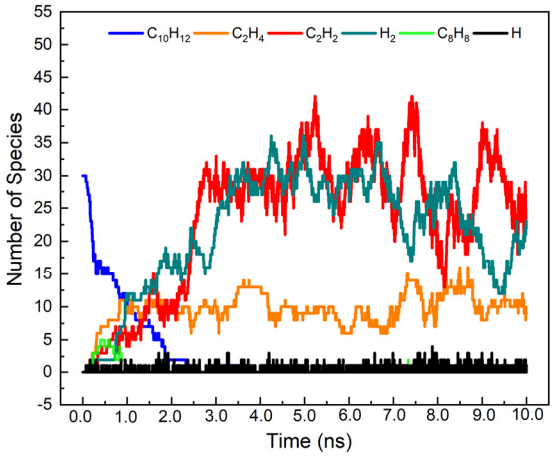

Fig. S23 Products distribution of the second parallel simulation beginning from the $C_{10}H_{12}$(30) system at 2000 K as a function of time.

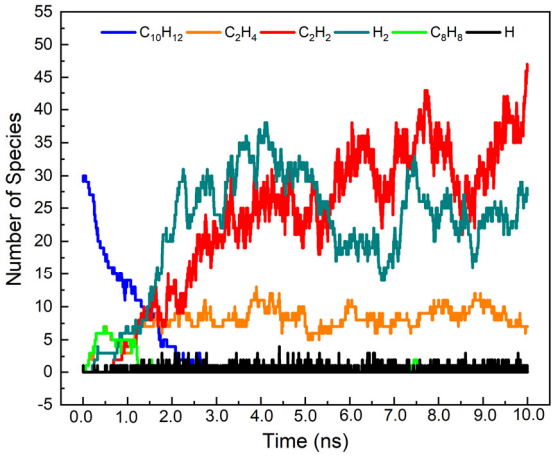

Fig. S24 Products distribution of the third parallel simulation beginning from the $C_{10}H_{12}$(30) system at 2000 K as a function of time.